HHS Public Access

Author manuscript

Asbestos Other Elongate Miner Part (2021). Author manuscript; available in PMC 2023 May 18.

Published in final edited form as:

Asbestos Other Elongate Miner Part (2021). 2021 ; 1632: 265–280. doi:10.1520/stp163220200067.

Size Separation of Amosite by Filtration and Shaking Methods

Taekhee Lee[1], **Rachel Walker**[1], **Jon Hummer**[1], **Elizabeth Ashley**[2], **Steven Mischler**[1]

[1]Centers for Disease Control and Prevention, National Institute for Occupational Safety and Health, Pittsburgh Mining Research Division, Health Hazards Prevention Branch, 626 Cochrans Mill Rd., Pittsburgh, PA 15236, USA

[2]Chemical and Biological Monitoring Branch, Health Effects Laboratory Division, National Institute for Occupational Safety and Health, Centers for Disease Control and Prevention, Cincinnati, OH 45213, USA

Abstract

The objectives of this study are (1) to separate fibrous grunerite (amosite) by its length using filtration and shaking techniques utilized in a previous study and (2) to create two distinct length groups (short and long) of the amosite with higher output in a cost-effective way. The shaking system included an electrodynamic exciter, a linear power amplifier, and an audio-frequency signal generator and was attached to a cowl sampler as a funnel loaded with a polycarbonate filter. A suspension of amosite was passed through the 10-μm pore size polycarbonate filter in the shaking system and was transferred to a filtration system through five different pore sizes of polycarbonate membrane filters in series from the top: 10-, 5-, 2-, 1-, and 0.2-μm pore sizes. Each polycarbonate filter was tightly clamped with two conductive 25-mm spacers with a 25-mm stainless steel support screen to prevent leakage. The amosite length and diameter were manually measured with images from a field emission scanning electron microscope (FESEM). A sequence of fields was selected at random locations, and an image of each field was acquired. The length and width of approximately 500 fibers for each sample were measured with ImageJ software. Two significantly different length groups (short and long) of amosite were collected (p <0.05). Approximately 95% of separated amosite (n = 499) using the filtration system were shorter than 5 μm (short fiber group), and approximately 80% of separated amosite (n = 503) using the shaking system were longer than 5 μm (long fiber group).

Keywords

amosite; asbestos; elongate mineral particles; length separation

Introduction

Inhalation exposure to respirable asbestiform elongate mineral particles (EMPs) leads to chronic fibrotic lung disorders, cancer, including malignant mesothelioma, and other

noncarcinogenic outcomes.[1,2] This signifies a substantial healthcare and economic burden worldwide. The National Institute for Occupational Safety and Health (NIOSH) published a report, titled “Asbestos Fibers and Other Elongate Mineral Particles: State of the Science and Roadmap for Research,” to outline a research agenda and projects for asbestos fibers and other EMPs.[3] The report recommended further research to understand health risks associated with exposure to EMPs, including asbestiform, nonasbestiform, and cleavage fragments. Currently, the Pittsburgh Mining Research Division (PMRD) is planning to obtain and characterize respirable fractions of 12 different EMPs. The test materials include the six regulated asbestos minerals—actinolite, amosite, anthophyllite, chrysotile, crocidolite, and tremolite, as well as their nonasbestiform analogues—actinolite, grunerite, anthophyllite, antigorite, riebeckite, and tremolite, respectively.

It would be desirable if these materials have similar physical characteristics for toxicological evaluations (e.g., similar length distributions by separation). Our first investigation[4] was to separate airborne glass fiber aerosols using commercially available instruments, the Aerodynamic Aerosol Classifier (AAC) and the multicyclone sampling array. The study concluded that glass fiber aerosols separation using the AAC might be able to produce two distinct length fiber groups (short and long) for toxicology evaluations. The production rate was similar to a previously published technique involving separation by dielectrophoretic mobility,[5–8] which is a limited amount for the toxicological evaluations. In addition, the decontamination process of the instrument is difficult and may create an exposure risk for laboratory personnel. Therefore, alternative methods were necessary to overcome these disadvantages. Spurny et al. showed three different techniques for separating asbestos for biological experiments, including (1) metallic micro-sieves for sieving in air, (2) nuclepore filters for filtration in liquid, and (3) a complex procedure, involving a knife mill, vibrating bed aerosol generator, cyclone, and sedimentation cylinder.[9] The study concluded that the techniques were promising for size separation of chrysotile, crocidolite, amosite, and glass fiber aerosols. These prepared materials were utilized in different studies.[10–12]

The present study is our second investigation (1) to separate EMP (amosite) by its length using similar techniques utilized in the Spurny et al. study[9] (e.g., filtration and shaking), and (2) to create two distinct length groups (shorter than 5 μm and longer than 5 μm) of the EMPs with higher output in a cost-effective way.

Materials and Methods

FIBROUS GRUNERITE (AMOSITE)

Fibrous grunerite, known as amosite from the asbestos mines of South Africa, was utilized in the present study, and the reference material was prepared by NIOSH in 1979.[13] It was described in the NIOSH publication as “GF-38, Ward’s Natural Science Establishment, Lyndenburg, South Africa.” According to NIOSH,

> This specimen, supplied as large rocks containing rows of fiber bundles perpendicular to plates of massive, nonfibrous mineral, exhibited true fibrous structure. Contaminants present included micaceous minerals (less than 4%), carbonates (less than 5%), magnetite (less than 2%) and isotropic minerals (less

than 1%). Thin section analysis demonstrated the presence of dense masses of fiber, with sparse biotite, iron oxide (magnetite), small masses of silicate minerals (possibly hornblende), and a trace of calcite. The geological occurrence of fibrous grunerite is in banded ironstone formations of Precambrian age. Accompanying minerals are magnetite, quartz, and grunerite and cummingtonite prisms, as well as carbonate and alteration products, such as nontronite. The precise geographic location from which this sample was obtained is not known. Its general source was the Lyndenburg-Petersburg belt in the Transvaal, South Africa. The material was processed by a centrifugal Knife Mill.

SEPARATION WITH SHAKING AND FILTRATION SYSTEM

A combination method of shaking and filtration was utilized to separate amosite. The experimental setup of the shaking system is shown in figure 1. A suspension of the amosite in type II pure water was placed in a cowl sampler as a funnel with a 10-μm pore size polycarbonate filter, and the polycarbonate filter was tightly clamped with two conductive 25-mm half-inch spacers with a 25-mm stainless steel support screen to prevent leakage. The assembly of the cowl, polycarbonate filter, and filter holder was submerged in a clean laboratory beaker filled with pure water. An electrodynamic exciter whose signal was amplified by a linear power amplifier was vibrated at 100 Hz with an audio-frequency signal generator. To transmit the vibration from the shaker to the assembly of cowl, an interface block was printed with a 3D printer. The interface block was connected to the shaker with a stinger rod. To determine shaking amplitude, an accelerometer was attached to the 3D printed interface block, and the signal was measured with an oscilloscope through an ICP sensor signal conditioner. The amosite concentration in pure water was 4 mg/mL, and a total of 10 mL suspension was used for the shaking system and sonicated about 20 min before adding to the shaking system. Each 1 mL of suspension was added with time intervals and pure water was added together while shaking. Fibers in the suspension, which were passed through the 10-μm polycarbonate filter in the shaking system, were transferred to a filtration system with five different pore sizes of polycarbonate membrane filters in series—from the top 10-, 5-, 2-, 1-, and 0.2-μm pore sizes (fig. 2). Each cowl sampler loaded with a polycarbonate filter stage was filled with pure water and the amosite suspension was added to the top of the filtration system when the water level was in the middle of the cowl with a 10-μm pore size polycarbonate filter. No vacuum was applied to the filtration system, and the filtered water was drained to a laboratory flask by gravity. Particle sizes were initially checked for each size of polycarbonate filters with a phase contrast microscope (PCM). When more than 50% of short fibers were observed in the large pore sizes of the polycarbonate filter (10 and 5 μm), the filters were vortex mixed and sonicated in pure water, and filtration was repeated at least five times.

SEPARATION WITH SHAKING

The separation with shaking system entailed shaking with different pore sizes of polycarbonate filters without the previously described filtration system, that is, one individual pore size polycarbonate filter at a time. A suspension of the amosite in pure water was placed in a cowl sampler (as a funnel) with a 10-μm pore size polycarbonate filter, and the filter holder was submerged in a clean laboratory beaker filled with pure water

during shaking with 100 Hz and peak-to-peak displacement that ranged from 0.31 to 0.36 mm. Fibers in the suspension passed through the 10-μm polycarbonate filter in the shaking system and were transferred to a 5-μm pore size polycarbonate filter with shaking. The process was repeated with 2.0-, 1.0-, 0.6-, and 0.4-μm pore size polycarbonate filters. The final suspension through the 0.4-μm pore size polycarbonate filter was collected on a 0.2-μm pore size polycarbonate filter using a filtration apparatus. The shaking procedure for each pore size filter was repeated three times by washing collected materials with vortex mix and sonication in pure water. Finally, shaking with a 1.0-μm pore size polycarbonate filter was repeated for additional separation of short amosite.

Both filtration and shaking procedures were conducted inside a ductless fume hood equipped with high-efficiency particulate air (HEPA) filters.

FIBER DIAMETER AND LENGTH MEASUREMENTS

Each size-separated amosite was placed in a centrifuge tube, 10 mL of pure water was added, and vortex mixed and sonicated to wash off the fibers from the polycarbonate filter. The number of fibers in each sample was measured using a PCM, and the samples were diluted or concentrated to make approximately 50 fibers/field for scanning electron microscope analysis with an assumption of 2000 × magnification. Each sample was then coated with a thin layer of gold/palladium utilizing a sputter coater. A sequence of fields was selected at random locations and an image of each field was acquired using a field emission scanning electron microscope (FESEM). The length and width of approximately 500 fibers for each sample were manually measured with ImageJ software, from the National Institutes of Health.[14]

AERODYNAMIC DIAMETER CALCULATION

The aerodynamic diameter of a fiber may be a good criterion to determine if that fiber is in respirable fraction. Fiber aerodynamic diameter depends on the fiber physical dimensions (diameter [d_f] and length [L]) and on the orientation of the fiber in the measuring flow field.[15,16] The aerodynamic diameter of the amosite was calculated with the fiber diameter and length measured by the FESEM using the following equations:

$$d_{ae,\parallel} = d_f\left\{\frac{9\rho_f}{4\rho_0}[\ln(2\beta) - 0.807]\right\}^{\frac{1}{2}}, \quad (1)$$

$$d_{ae,\perp} = d_f\left\{\frac{9\rho_f}{8\rho_0}[\ln(2\beta) + 0.193]\right\}^{\frac{1}{2}}, \quad (2)$$

where:

$d_{ae,\parallel}$ = aerodynamic diameter when the fiber is parallel to relative gas motion,

$d_{ae,\perp}$ = aerodynamic diameter when the fiber is aligned perpendicular to relative gas motion,

$\beta = \frac{L}{d_f}$ = the aspect ratio, and

ρ_f and ρ_0 = the fiber (3450 Kg/m^3) and unit densities, respectively.

For random orientation, the aerodynamic diameter was calculated as follows:

$$d_{ae} = \frac{(d_{ae,\parallel} + 2d_{ae,\perp})}{3} \quad (3)$$

Results and Discussion

SEPARATION WITH FILTRATION SYSTEM

The FESEM images of the amosite separated with the filtration system are shown in figure 3. Long and short amosite fibers were observed together in the large pore sizes stages of the polycarbonate filters (10 and 5 μm) in the filtration system, but only short fibers were observed in the last stage (0.2–μm pore size) of the filtration system. The cumulative length fractions of the amosite separated with the filtration system are shown in figure 4, and descriptive statistics are shown in table 1. The length of the separated amosite ranged from 0.08 to 71.43 μm. Fibers longer than 100 μm were not found because the long fibers were removed from the shaking system (10-μm pore size polycarbonate filter) before the filtration system. Mean and geometric mean length of the separated amosite were not linearly increased when the polycarbonate filter pore size was increased because short fibers were not completely separated from the long fibers in the filtration system. For the fibers captured on the smaller pore sizes of the filtration systems, approximately 95% of measured amosite fibers (n = 499) were shorter than 5 μm (table 1), and these may be utilized as a short fiber group for a toxicological evaluation. It would be difficult to obtain long fiber samples (> 5μm) by separating the short fibers and long fibers in the filtration system because shorter fibers are generally dominant in their size distribution.[17] All fiber-length data sets from the filtration systems failed the normality test (Shapiro-Wilk test), and the Kruskal-Wallis one-way analysis of variance on ranks (median value comparison) was used to compare each sample. The samples from the 0.2-μm pore size polycarbonate filter were statistically different in length ($p < 0.05$) when compared to samples from the 1-, 2-, and 10-μm pore size polycarbonate filters. The samples from the 0.2- and 5-μm pore size polycarbonate filters were not statistically different ($p > 0.05$). The cumulative length fractions of 0.2- and 5-μm pore size polycarbonate filters were similar to each other up to a fiber length of 5 μm (fig. 4). Diameters of separated amosite ranged from 0.01 to 3.2 μm, and the calculated aerodynamic diameters, using equations (1) to (3), ranged from 0.15 to 12.67 μm. The 95th percentile aerodynamic diameters from the 0.2- and 10-μm pore size polycarbonate filters were 1.99 and 4.24 μm, respectively, and the samples might both be included in the respirable fraction. The normalized aerodynamic diameter distribution of each pore size of polycarbonate filter for the filtration system is shown in figure 5.

SEPARATION WITH SHAKING SYSTEM

The FESEM images of amosite fibers separated with the shaking system are shown in figure 6, and cumulative length fractions for different pore sizes of the polycarbonate filters are

shown in figure 7. Descriptive statistics of the amosite separated with the shaking system are shown in table 2. A large number of short fibers were not observed in large pore sizes of the polycarbonate filter in the shaking system compared with that from the filtration system. The SEM images and cumulative plot show that approximately 80% of the samples with the small size pore size filters (0.6, 0.4, and <0.4 μm) in the shaking system were shorter than 5 μm, indicating that the filtration system (~95%) would be better to collect the fibers <5 μm. Approximately 80% of the samples with a 2.0-μm pore size polycarbonate filter were longer than 5 μm, and a 25% percentile was 5.57 μm (table 2), which may be utilized as a long fiber group for a toxicological evaluation. All fiber length data sets from the shaking system failed the normality test (Shapiro-Wilk test), and the Kruskal-Wallis one-way analysis of variance on ranks (median value comparison) was used to compare each sample. Most of the pairs of the group showed significant differences, except pairs of 2-μm versus 10-μm pore size, first 1-μm versus second 1-μm pore size, 0.6-μm versus 0.4-μm, and 0.4-μm versus <0.4-μm pore size. Based on the findings from the present study, two distinct length groups of fibers might be collected when utilizing the filtration and shaking systems—a short fiber group (<5 μm) with the filtration system and a long fiber group (>5 μm) with the shaking system. Figure 8 shows a cumulative plot of short and long fiber groups from each method, and the length of the two groups were significantly different in accordance with the Mann-Whitney Rank Sum Test (p <0.05). Diameters of the amosite separated with the shaking system ranged from 0.1 to 13 μm, and calculated aerodynamic diameters using equations (1) to (3) ranged from 0.3 to 45 μm. The 95th percentile aerodynamic diameters from the <0.4-μm and 10-μm pore size polycarbonate filter with the shaking system were 2.65 and 10.7 μm, respectively, and not all the samples with a 10-um pore size polycarbonate filter might be considered to be a respirable fraction. The normalized aerodynamic diameter distribution of each pore size of polycarbonate filter for the shaking system is shown in figure 9. Relatively smaller length, diameter, and aerodynamic diameters of amosite were observed in the filtration system because long and thick amosite were screened out before adding into the filtration system.

The filtration system in liquids utilized in Spurny et al.[9] had a filter battery for removing large-size fibers, a cylinder for holding the suspension, two or more nuclepore filters in series, a vibration system, and a vacuum pump that was applied to the system to have a flow rate of 0.7 L/h. Their optimal frequencies for glass fiber separation were from 80 to 120 Hz and the amplitude was 0.3 mm, which is similar to the present study. Spurny et al. showed that the percentage of fibers (glass fibers and chrysotile) <5 μm were from 0.8% to 4.6%. Approximately 98% of the fibers (amosite, chrysotile, crocidolite, and glass fiber) from the multiple procedures were <3 μm in length in the very fine fraction groups.[9] The percentage fibers <5 μm were similar between Spurny et al. and the present study (~95%). The shaking procedure was repeated three times in the present study for all pore sizes of the polycarbonate filters. If the shaking procedure was repeated more than three times, it might be expected that more fibers <5 μm could be removed from the long fiber group.

Both filtration and shaking separation systems are relatively inexpensive compared with the instrument utilized in our first investigation.[4] Employing multiple units of both systems and larger diameter (47 mm) of the polycarbonate filter can shorten the collection time of these materials for toxicological evaluations. Another advantage of the systems is that laboratory personnel exposure to the toxic materials is less likely or very minimal because of their wet

procedure. Personal and area air monitoring in accordance with the NIOSH 7400 method.[18] was conducted during separation, and no fibers were identified in the laboratory air. Samples separated by fiber length using a pore size polycarbonate filter should be checked with the PCM for quality control before combining the samples. In addition, the respirable fraction of the EMPs should be collected before the procedures of the shaking or filtration. Utilization of respirable size-selective samplers operating at higher flow rates[19,20] and the vortex mixer shaking fiber generation method[4,21,22] might shorten the collection time for the respirable fraction.

In the present study, a total of 6,567 fibers were measured manually for both length and diameter, which is a limited measurement and a labor-intensive method. A faster and more accurate fiber length and diameter measurement method would be helpful to determine particle size distribution of the separated fibers. Cho et al. showed the capability of an automatic counting of asbestos fibers (high-throughput microscopy), although the study focused on fiber counting rather than on reporting fiber length or diameter information.[23] In addition, differential interference contrast microscopy might be able to reduce fiber counting and detection time by increasing the contrast.[24] Cossio et al. reported an unattended SEM-energy dispersive X-ray (EDS) asbestos analysis method, and the study showed high precision and reproducibility, which can reduce analytical time (maximum 2 h/sample).[25]

Conclusions

This study was the second investigation to separate EMPs (amosite) by length using shaking and filtration techniques as previously reported. The final output materials for the toxicological evaluation is expected to be larger than the one from our first investigation. Although the filtration and shaking methods are labor intensive, both systems have advantages. They are relatively inexpensive, decontamination of the equipment is not difficult, and laboratory personnel exposure to toxic materials is likely minimized because of the wet procedures of these methods. By utilizing both methods, short (<5 μm) and long (> 5 μm) fibers can be collected utilizing the filtration and shaking methods, respectively. Removing short fibers from the long fiber group and removing long fibers from the short fiber group are likely achievable by repeating these procedures.

FUNDING

National Institute for Occupational Safety and Health, Project #9390BMJ: Understanding elongate mineral particle exposure in mining.

References

1. Lippmann M, “Toxicological and Epidemiological Studies on Effects of Airborne Fibers: Coherence and Public [Corrected] Health Implications,” Critical Reviews in Toxicology 44, no. 8 (2014): 643–695. [PubMed: 25168068]
2. Oberdörster G and Graham U, “Predicting EMP Hazard: Lessons from Studies with Inhaled Fibrous and Non-fibrous Nano- and Micro-particles,” Toxicology and Applied Pharmacology 361 (2018): 50–61. [PubMed: 29751048]
3. Asbestos Fibers and Other Elongate Mineral Particles: State of the Science and Roadmap for Research, Current Intelligence Bulletin 62, DHHS Publication No. 2011-159 (Washington, DC:

Department of Health and Human Services, National Institute for Occupational Safety and Health, 2011).

4. Lee T, Ku BK, Walker R, Kulkarni P, Barone T, and Mischler S, "Aerodynamic Size Classification of Glass Fiber Aerosols," Journal of Occupational and Environmental Hygiene 17, no. 6 (2020): 301–311. [PubMed: 32294024]
5. Baron PA, Deye GJ, and Fernback J, "Length Separation of Fibers," Aerosol Science and Technology 21, no. 2 (1994): 179–192.
6. Blake T, Castranova V, Schwegler-Berry D, Baron P, Deye GJ, Li C, and Jones W, "Effect of Fiber Length on Glass Microfiber Cytotoxicity," Journal of Toxicology and Environmental Health, Part A, 54 (1998): 243–259. [PubMed: 9638898]
7. Deye GJ, Gao P, Baron PA, and Fernback J, "Performance Evaluation of a Fiber Length Classifier," Aerosol Science and Technology 30, no. 5 (1999): 420–437.
8. Zeidler-Erdely PC, Calhoun WJ, Ameredes BT, Clark MP, Deye GJ, Baron P, Jones W, Blake T, and Castranova V, "In Vitro Cytotoxicity of Manville Code 100 Glass Fibers: Effects of Fiber Length on Human Alveolar Macrophages," Particle and Fibre Toxicology 3, no. 5 (2006), 10.1186/1743-8977-3-5
9. Spurny KR, Stober W, Opiela H, and Weiss G, "Size-Selective Preparation of Inorganic Fibers for Biological Experiments," American Industrial Hygiene Association Journal 40, no. 1 (1979): 20–38. [PubMed: 484448]
10. Oberdörster G, Morrow PE, and Spurny K, "Size Dependent Lymphatic Short Term Clearance of Amsite Fibres in the Lung," Annals of Occupational Hygiene 32, Suppl. 1 (1988): 149–156.
11. Pott F, Ziem U, Reiffer FJ, Huth F, Erns H, and Mohr U, "Carcinogenicity Studies on Fibres, Metal Compounds, and Some Other Dusts in Rats," Experimental Pathology 32, no. 3 (1987): 129–152. [PubMed: 3436395]
12. Spurny KR, "Measurement and Analysis of Chemically Changed Mineral Fibers after Experiments in Vitro and in Vivo," Environmental Health Perspectives 51 (1983): 343–355. [PubMed: 6315377]
13. Preparation and Characterization of Analytical Reference Minerals, Department of Health, Education, and Welfare (NIOSH) Publication No. 79-139 (Washington, DC: Department of Health and Human Services, National Institute for Occupational Safety and Health, 1979).
14. Schneider CA, Rasband WS, and Eliceiri KW, "NIH Image to ImageJ: 25 Years of Image Analysis," Nature Methods 9, no. 7 (2012): 671–675. [PubMed: 22930834]
15. Cox RG, "The Motion of Long Slender Bodies in a Viscous Fluid Part 1. General Theory," Journal of Fluid Mechanics 44 (1970): 791–810.
16. Baron PA and Willeke K, Aerosol Measurement, Principles, Techniques, and Applications, 2nd ed. (New York: Wiley, 2001).
17. Chatfield EJ, "Measurement of Elongate Mineral Particles: What We Should Measure and How Do We Do It?", Toxicology and Applied Pharmacology 361 (2018): 36–46. [PubMed: 30134140]
18. "Asbestos and Other Fibers by Phase Contrast Microscopy (PCM)," NIOSH Method 7400, in NIOSH Manual of Analytical Methods, 4th ed. (Washington, DC: U.S. Department of Health and Human Services, 1994)
19. Lee T, Kim SW, Chisholm WP, Slaven J, and Harper M, "Performance of High Flow Rate Samplers for Respirable Particle Collection," Annals of Occupational Hygiene 54 (2010): 697–709. [PubMed: 20660144]
20. Lee T, Thorpe A, Cauda E, Tipton L, and Echt A, "Laboratory Comparison of New High Flow Rate Respirable Size-Selective Sampler," Journal of Occupational and Environmental Hygiene 15, no. 10 (2018): 755–765. [PubMed: 30095363]
21. Ku BK, Deye G, and Turkevich LA, "Characterization of a Vortex Shaking Method for Aerosolizing Fibers," Aerosol Science and Technology 47, no. 12 (2013): 1293–1301. [PubMed: 26635428]
22. Ku BK, Deye G, and Turkevich LA, "Screen Collection Efficiency of Airborne Fibers with Monodisperse Length," Journal of Aerosol Science 115 (2017): 250–262.

23. Cho M, Yoon S, Han H, and Kim JK, “Automated Counting of Airborne Asbestos Fibers by a High-Throughput Microscopy (HTM) Method,” Sensors 11 (2011): 7231–7242. [PubMed: 22164014]

24. Zarubiieva I, Hwang GB, Lee JS, Bae G-N, Oh Y-M, Park S-W, Lee TJ, Lee HJ, Woo DH, Lee S, Cho M-O, Kim JK, Jun SC, and Kim JH, “Asbestos Imaging and Detection with Differential Interference Contrast Microscopy,” Aerosol and Air Quality Research 13 (2013): 1145–1150.

25. Cossio R, Albonicoc C, Zanellac A, Fraterrigo-Garofalod S, Avataneoe C, Compag- nonia R, and Turci F, “Innovative Unattended SEM-EDS Analysis for Asbestos Fiber Quantification,” Talanta 190 (2018): 158–166. [PubMed: 30172493]

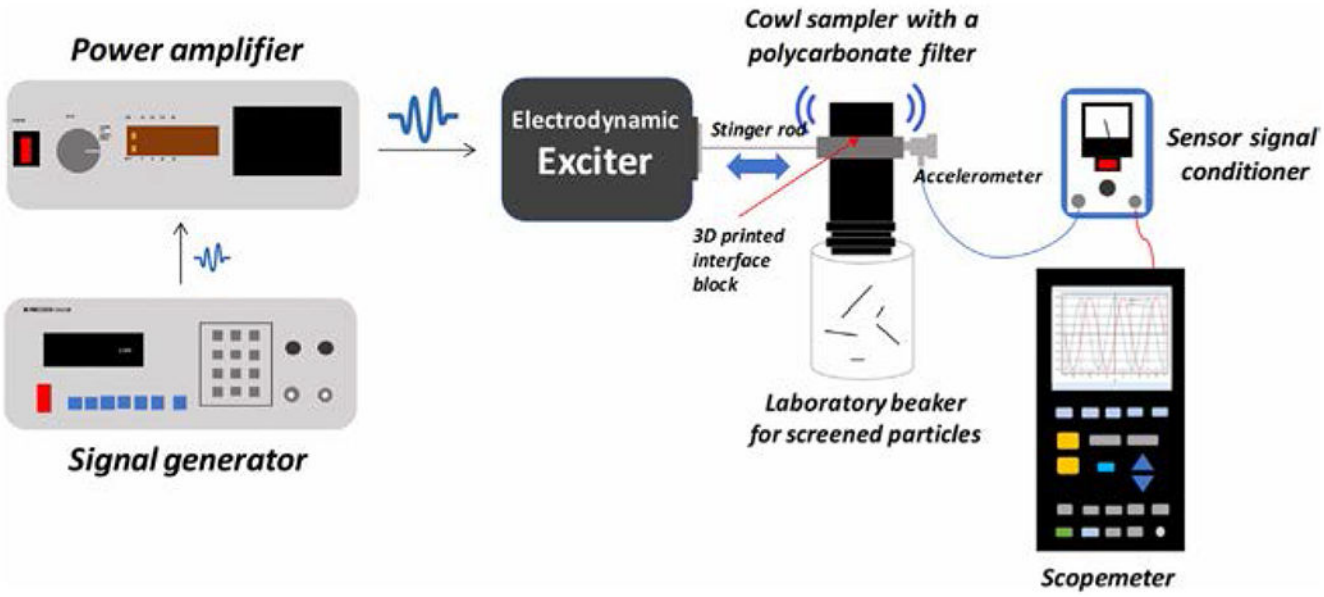

FIG. 1.
Experimental setup for elongate mineral particle separation with shaking system.

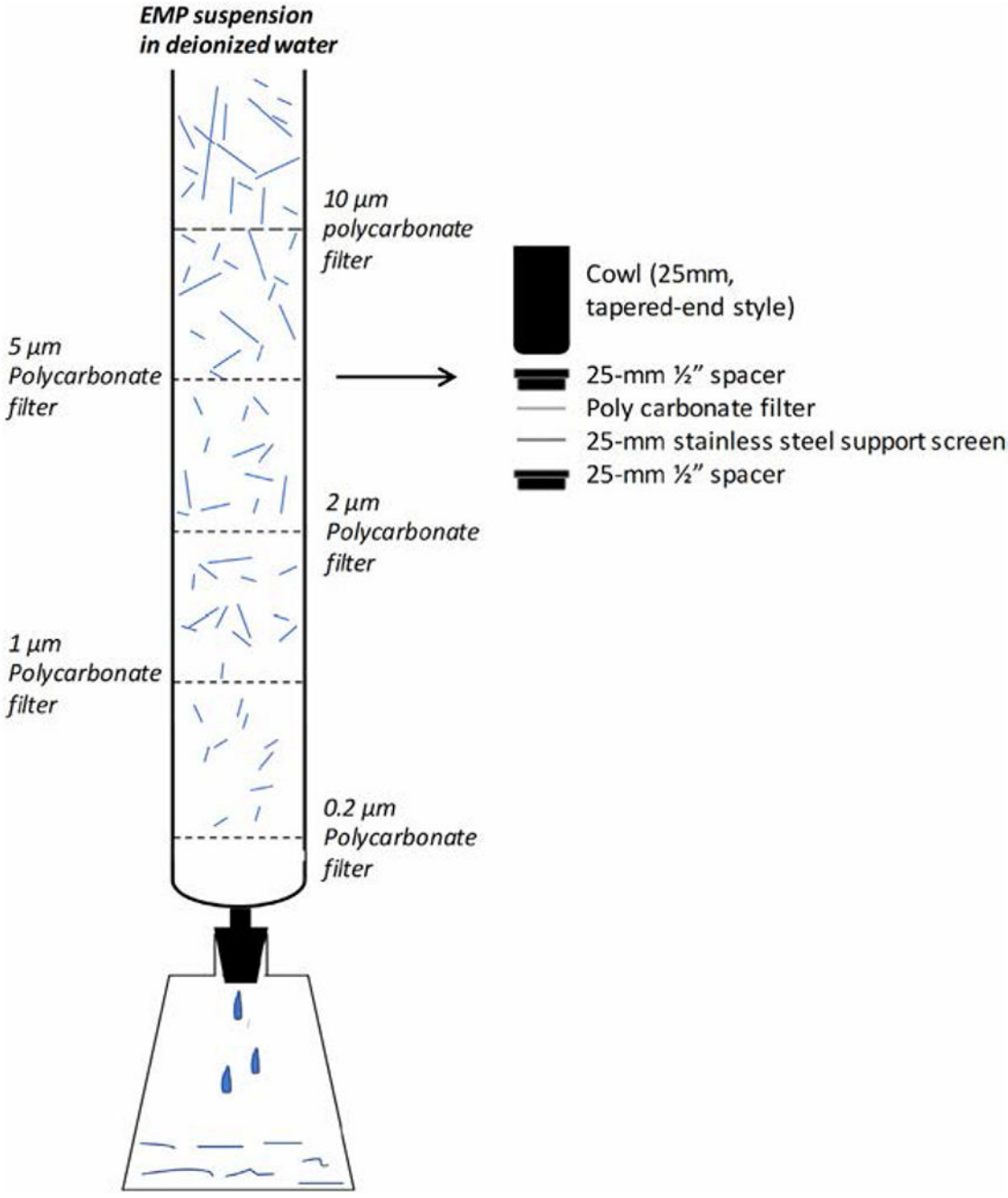

FIG. 2.
Experimental setup for elongate mineral particle separation with filtration system.

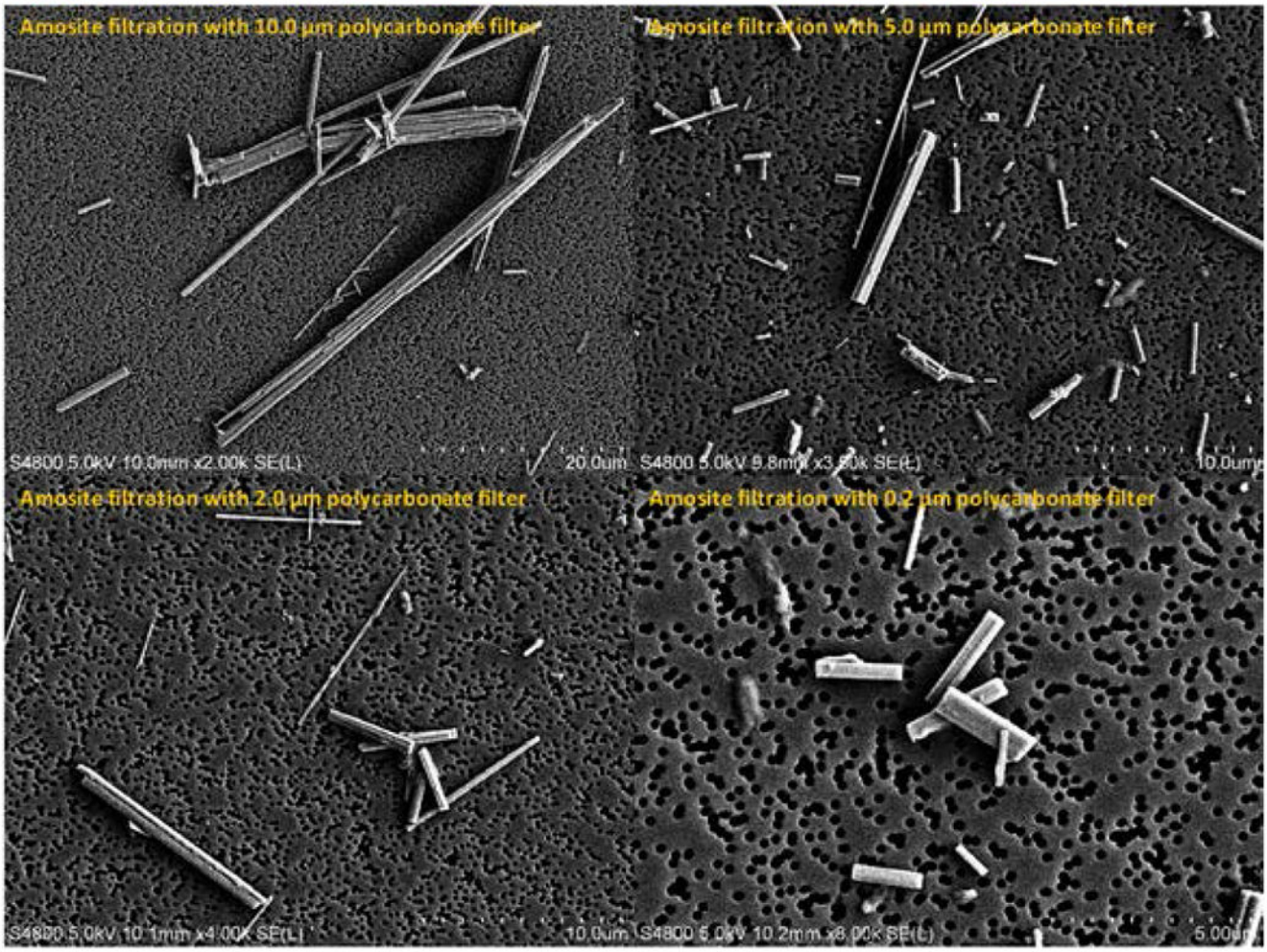

FIG. 3.

Field emission scanning electron microscope images of amosite separated with the filtration method (10.0-, 5.0-, 2.0-, and 0.2-µm pore size polycarbonate filters). Please note that the magnification of each image is different.

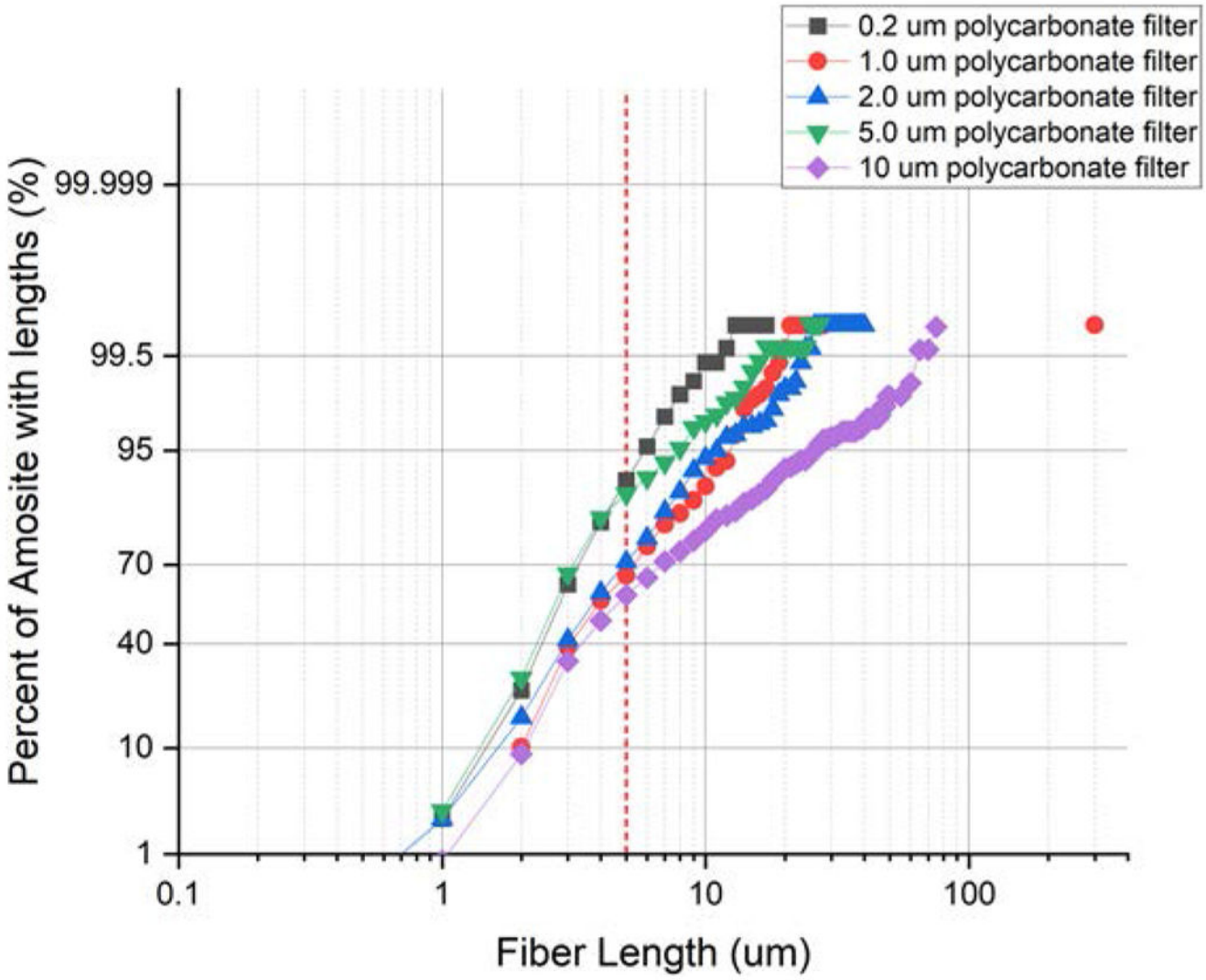

FIG. 4.
Cumulative length fractions of the separated amosite with filtration system.

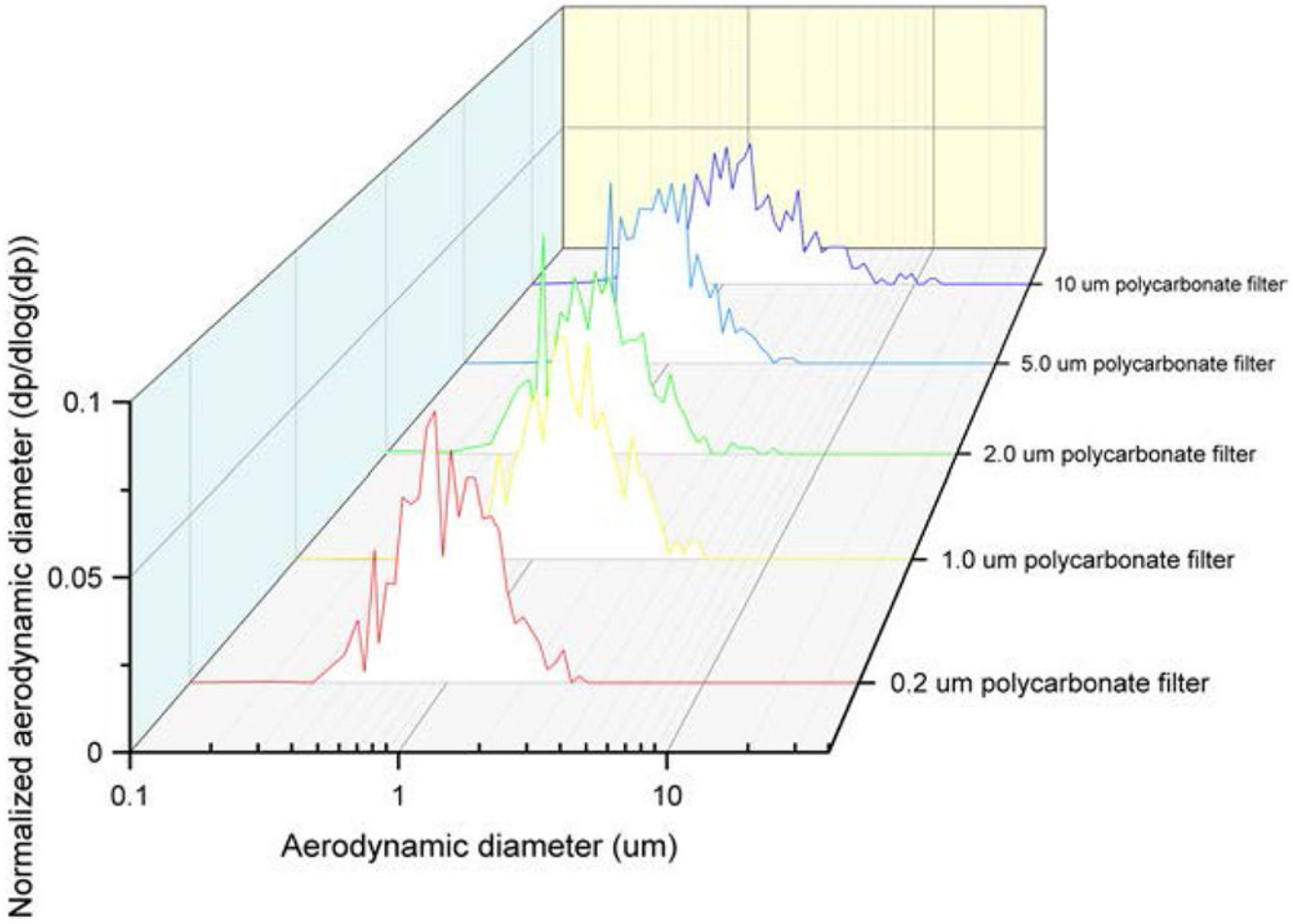

FIG. 5.
Normalized aerodynamic diameter distribution of the filtration system.

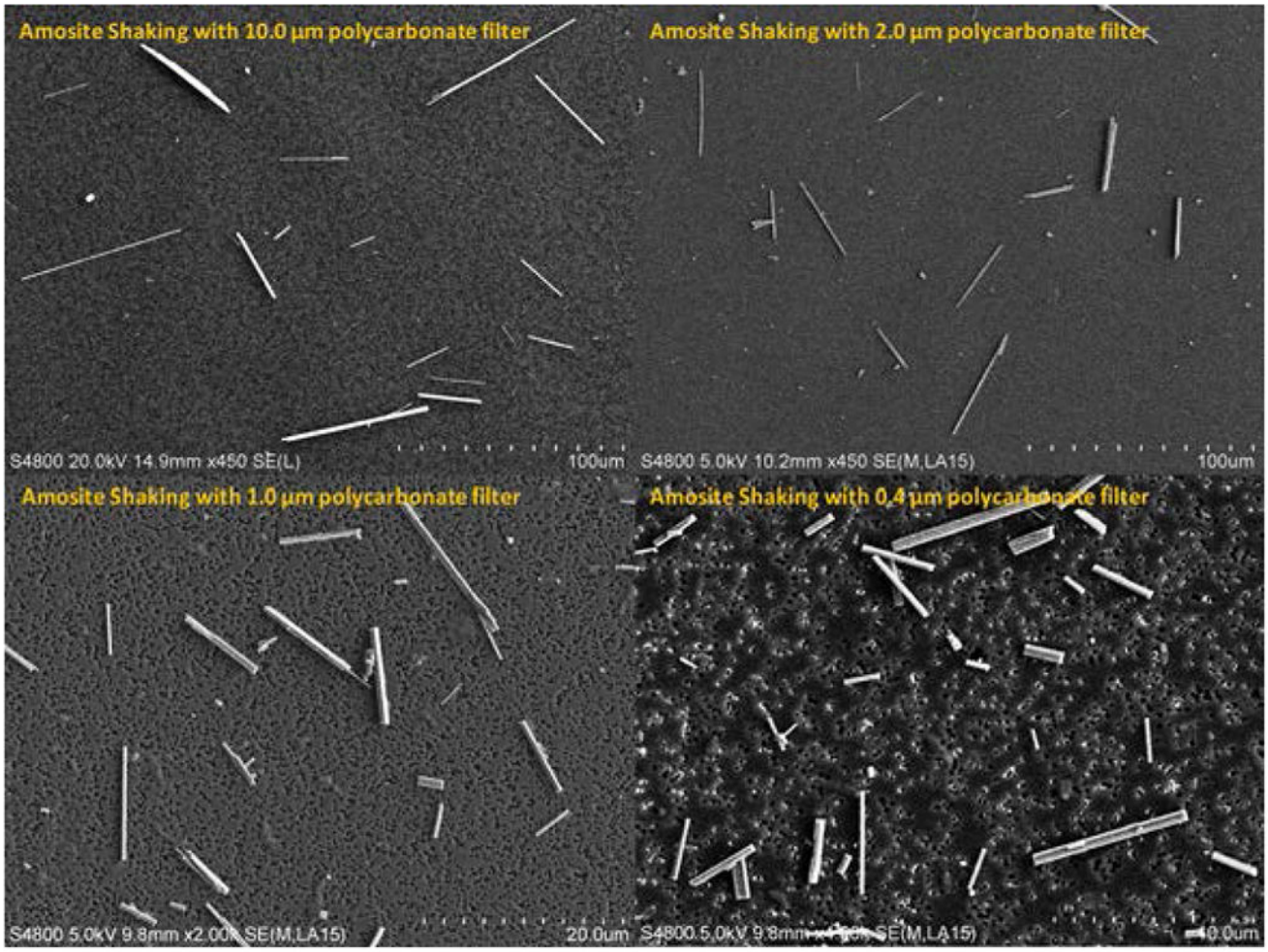

FIG. 6.

Field emission scanning electron microscope images of amosite separated with the shaking method (10.0-, 2.0-, 1.0-, and 0.4-µm pore size polycarbonate filters). Please note that the magnification of each image is different.

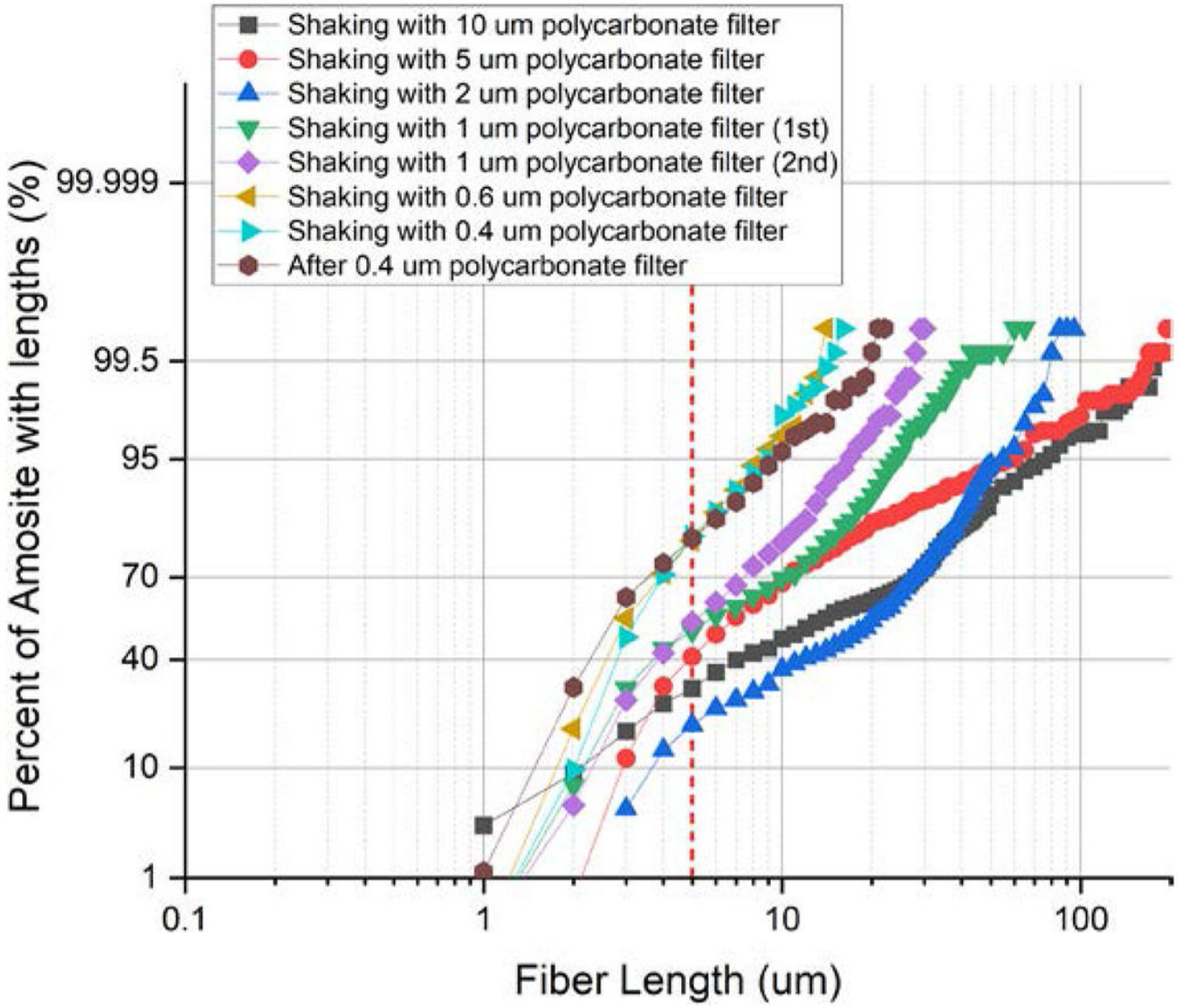

FIG. 7.
Cumulative length fractions of the separated amosite with shaking system.

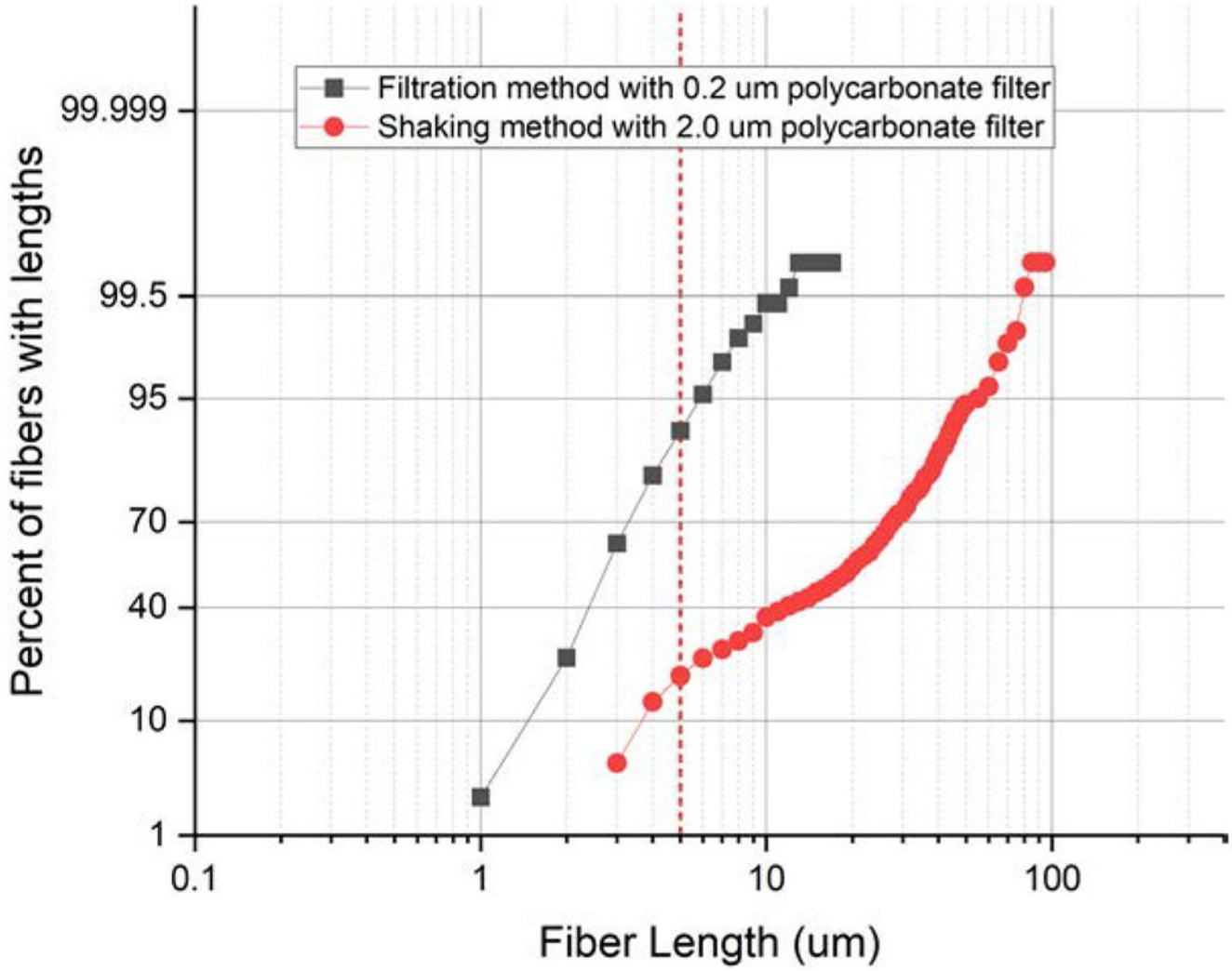

FIG. 8.
Cumulative length fraction of the separated amosite with filtration (shortest group) and shaking system (longest group).

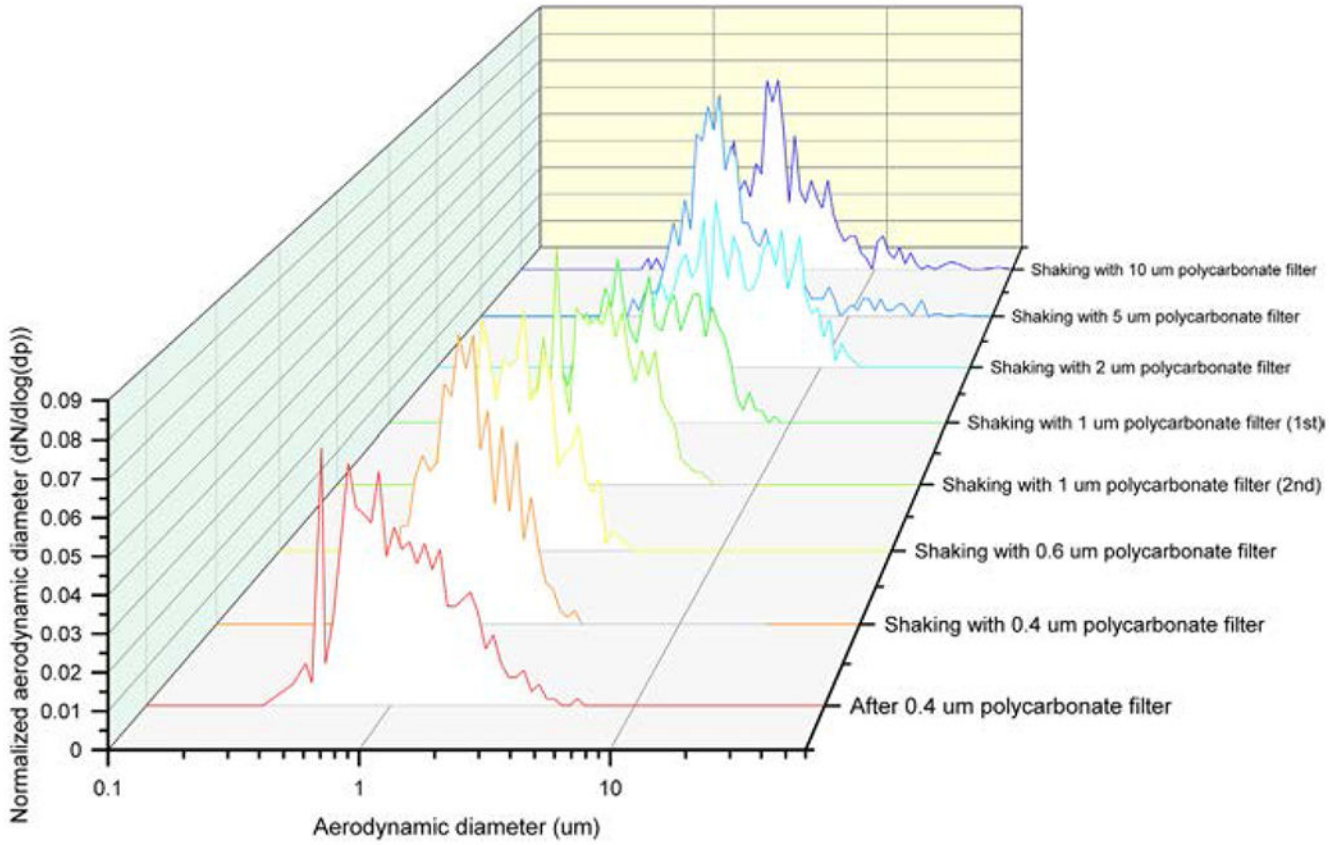

FIG. 9.
Normalized aerodynamic diameter distribution of the shaking system.

TABLE 1

Descriptive statistics of separated amosite using filtration method

		Polycarbonate Pore Size, μm				
		0.2	**1**	**2**	**5**	**10**
Fiber length (μm)	N[a]	499	500	501	520	478
	Mean	2.03	3.85	3.57	2.19	6.69
	SD[b]	1.60	3.48	3.86	2.55	9.99
	GM[c]	1.63	2.77	2.41	1.58	3.57
	GSD[d]	1.90	2.23	2.44	2.10	2.86
	Minimum	0.38	0.53	0.08	0.30	0.40
	25%	1.02	1.48	1.30	0.93	1.57
	Median	1.56	2.52	2.40	1.46	3.05
	75%	2.46	4.95	4.56	2.37	7.25
	95%	4.96	11.24	9.60	6.82	25.06
	Maximum	16.75	27.63	39.75	26.45	71.43
Fiber diameter (μm)	N[a]	499	500	501	520	478
	Mean	0.33	0.47	0.29	0.32	0.45
	SD[b]	0.14	0.22	0.19	0.15	0.38
	GM[c]	0.30	0.43	0.24	0.29	0.35
	GSD[d]	1.52	1.55	1.85	1.56	1.97
	Minimum	0.03	0.03	0.01	0.04	0.04
	25%	0.23	0.33	0.17	0.21	0.23
	Median	0.30	0.41	0.24	0.28	0.34
	75%	0.40	0.56	0.34	0.39	0.53
	95%	0.61	0.87	0.62	0.61	1.11
	Maximum	0.88	1.46	2.01	1.15	3.20
Aerodynamic diameter (μm)	N[a]	499	500	500	520	478
	Mean	1.07	1.58	1.02	1.03	1.65
	SD[b]	0.47	0.78	0.62	0.53	1.46
	GM[c]	0.98	1.42	0.87	0.93	1.28
	GSD[d]	1.53	1.60	1.80	1.58	1.99
	Minimum	0.15	0.15	0.03	0.18	0.18
	25%	0.73	1.02	0.64	0.67	0.81
	Median	0.97	1.38	0.88	0.90	1.20
	75%	1.31	1.92	1.26	1.20	2.00
	95%	1.99	3.07	2.06	2.13	4.24
	Maximum	3.15	4.79	5.61	4.00	12.67

[a] Measured sample number with scanning electron microscope.

[b] Standard deviation.

[c] Geometric mean.

[d] Geometric standard deviation.

TABLE 2

Descriptive statistics of separated amosite using shaking method

		Polycarbonate Pore Size, μm							
		<0.4	**0.4**	**0.6**	**1**	**1**	**2**	**5**	**10**
Fiber length (μm)	N[a]	513	507	513	508	515	503	505	505
	Mean	2.64	2.78	2.63	5.51	7.41	19.86	12.99	23.76
	SD[b]	2.99	2.24	2.26	5.04	8.08	16.38	23.96	30.46
	GM[c]	1.78	2.19	1.98	3.81	4.29	12.86	6.22	12.74
	GSD[d]	2.28	1.94	2.07	2.38	2.91	2.82	2.96	3.11
	Minimum	0.44	0.45	0.41	0.50	0.45	1.36	0.74	0.79
	25%	0.89	1.35	1.17	1.93	1.72	5.57	2.71	4.99
	Median	1.51	2.03	1.77	3.51	3.88	16.82	5.08	12.09
	75%	3.04	3.34	3.37	7.40	11.10	30.04	11.63	32.06
	95%	8.28	7.97	7.14	15.68	23.04	49.95	52.45	80.07
	Maximum	21.97	15.72	13.31	29.13	60.69	91.22	223.08	227.49
Fiber diameter (μm)	N[a]	513	507	513	508	515	503	505	505
	Mean	0.38	0.39	0.40	0.53	0.63	1.10	0.81	0.91
	SD[b]	0.20	0.15	0.17	0.25	0.36	0.71	0.99	1.03
	GM[c]	0.33	0.36	0.36	0.48	0.54	0.91	0.61	0.69
	GSD[d]	1.60	1.47	1.54	1.60	1.76	1.83	1.90	1.96
	Minimum	0.10	0.11	0.11	0.14	0.12	0.16	0.12	0.12
	25%	0.24	0.28	0.26	0.34	0.36	0.58	0.42	0.42
	Median	0.33	0.36	0.36	0.47	0.53	0.83	0.54	0.63
	75%	0.46	0.47	0.52	0.67	0.85	1.47	0.74	0.97
	95%	0.77	0.69	0.72	1.02	1.36	2.57	2.54	2.56
	Maximum	1.51	1.09	1.07	1.49	2.27	3.93	9.30	13.15
Aerodynamic diameter (μm)	N[a]	513	507	513	154	505	503	505	505
	Mean	1.24	1.29	1.28	1.91	2.24	4.24	3.01	3.68
	SD[b]	0.74	0.53	0.59	1.00	1.35	2.63	3.68	4.00
	GM[c]	1.07	1.19	1.16	1.68	1.88	3.52	2.22	2.77
	GSD[d]	1.68	1.48	1.56	1.68	1.83	1.86	1.95	1.99
	Minimum	0.32	0.40	0.36	0.50	0.45	0.65	0.48	0.51
	25%	0.71	0.91	0.83	1.16	1.17	2.18	1.48	1.70
	Median	1.01	1.17	1.14	1.67	1.86	3.46	1.94	2.57
	75%	1.53	1.61	1.59	2.61	3.08	5.84	2.85	4.09
	95%	2.65	2.33	2.49	3.89	4.78	9.28	9.06	10.70
	Maximum	5.80	3.41	3.56	5.47	8.29	13.94	37.99	45.07

[a]Measured sample number with scanning electron microscope.

[b]Standard Deviation.

[c]Geometric Mean.

[d]Geometric Standard Deviation